Iranian Journal of Fisheries Sciences 19(6) 3327-3344 2020
DOI: 10.22092/ijfs.2020.350833.0

Nanosilver-impregnated and acid-treated vermiculite within water filtration system and its dual function in bacterial disinfection and silver reabsorption

Salari Joo H.[1]; Kalbassi M.R.[1*]; Paknejad H.[2]

Received: December 2019 Accepted: February 2020

Abstract

Antibacterial activity of silver-impregnated vermiculite and silver removal capability of acid-treated vermiculite (Verm-A) were assessed through 4-stage water filtration systems. The antibacterial vermiculite was prepared through cation exchange process in silver nitrate solutions of 0, 500, 1000, and 2000 mgl^{-1}, named Verm-B_0, Verm-B_{500}, Verm-B_{1000}, and Verm-B_{2000}, respectively. The Verm-A was only treated with 1 M HCl to increase its negative zeta potential. Bacterium *Aeromonas hydrophila* was inoculated into the filtration systems and then total colony forming units in water samples was enumerated for 96 h. Flame atomic absorption spectrometer showed the maximum silver adsorption (49.17 mg/g) by Verm-B_{2000}. Scanning electron microscopy micrographs illustrated silver with nano dimension crystallites with the average sizes of 274.808, 194, 162.258 nm on the surface of Verm-B_{2000}, Verm-B_{500}, and Verm-B_{1000}, respectively. All the Verm-B products were approved to possess a strong antibacterial activity, with reducing the bacterial growth over 95% in all of the filtration systems containing Verm-$B_{500\text{-}2000}$. The highest log reduction value of 3.47 CFU mL^{-1} at 96 h was observed for the filtration system containing Verm-B_{1000}. The percentage of silver released from the total Ag in Verm-B_{500} was 32.36%, Verm-B_{1000} 27.87%, and Verm-B_{2000} 17.24%; of these amounts, 90.9%, 81.8%, and 75.7% were reabsorbed respectively, by Verm-A. The observed bactericidal efficiency could open an avenue to use silver-impregnated vermiculite in water treatment. Moreover, acid treated vermiculite could be introduced as an affordable absorbent for removal of silver from water filtration system, industrial wastewater and reduce metallic environmental contaminants.

Keywords: Silver nanoparticles, Vermiculite, Antibacterial, Water purification, Silver removal

1-Department of Fisheries, Faculty of Marine Sciences, Tarbiat Modares University, Noor, Mazandaran, Iran.

2-Department of Fisheries, Faculty of Fisheries and Environmental Sciences, Gorgan University of Agricultural Sciences and Natural Resources, Gorgan, Iran.

*Corresponding author's Email: kalbassi_m@modares.ac.ir

[DOR: 20.1001.1.15622916.2020.19.6.30.2]

Introduction

Currently, unsafe drinking water is the third leading risk factor for disease and is of great concern worldwide (Kirby *et al.*, 2017). Over one billion people lack access to improved water supplies, and not all improved sources are necessarily free of microbial contamination (Kirby *et al.*, 2017; Pompei *et al.*, 2017). It is estimated that over 600 million people rely on unsafe potable water contaminated during transport and storage with the majority residing in rural areas in developing countries (Lantagne *et al.*, 2010; Qu *et al.*, 2013; Singer *et al.*, 2017). Waterborne bacteria in drinking and washing waters increase the possibility of spreading a variety of infections, with consumption and contact being the main transmission routes (Khan and Ahmad, 2016). Therefore, from 1990 to 2012, global challenges to providing safe drinking water resulted in a 50% decrease in child mortality associated with low water quality for drinking, hygiene and sanitation (Abebe *et al.*, 2016).

Household water treatment technologies to improve water quality in poor communities have undergone significant development. The performance of water treatment devices is greatly improved by the use of materials with high anti-microbial characteristics, such as silver, as a primary water disinfectant (Benhacine *et al.*, 2016; Fewtrell *et al.*, 2017). Given their long-lasting biocidal activity, composites containing silver nanoparticles have captured attention in both academic and technologic fields. However, silver nanoparticles meet many limitations to become part of large-scale water treatment plants. The main drawbacks are related to the particle preparation cost and the cost of treatment operation with respect to increase in supplied water price for the consumers (Simeonidis *et al.*, 2016). A further problematic issue is the uncontrolled size and heterogeneity of the silver nanoparticles when mechanically mixing nanoparticles with polymer composites, and thus decreasing the point-of-time biocidal performance of the materials (Benhacine *et al.*, 2016).

Some natural clay minerals (e.g., montmorillonite, kaolinite, and vermiculite) with high cation exchange and negative surface capacities as well as large surface area have interesting absorption ability to be impregnated with antibacterial active metals (e.g., Ag^{+} and Cu^{2+}) through anchoring on their external surface and interlayer space (Benhacine *et al.*, 2016). The 2:1 layer clay minerals have been very convenient as substrates for the growth of metallic nanoparticles. Some studies suggested that these aluminosilicate minerals could open new avenues to develop new classes of antimicrobial materials (Valášková *et al.*, 2010; Drelich *et al.*, 2011). In the recent years, incorporation of low cost materials, such as ceramic, polymeric membrane, polyurethane, agricultural waste, and fiber, in household water treatment technology with proper

[DOR: 20.1001.1.15622916.2020.19.6.30.2]

disinfection effectiveness has been proposed to achieve the millennium development goals for water (Noubactep *et al.*, 2010; Praveena and Aris, 2015; Simeonidis *et al.*, 2016) . The incorporation of widely accessible and environmentally sustainable clay minerals by a water filter system would be a promising and cost-effective method to reduce or eliminate the pathogenic microorganisms and to provide safe water for human usage and consumption.

Vermiculite is an inexpensive clay mineral with a chemical formula of Mg, Ca 0.3–0.45 $(H_2O)n$ (Mg, Fe, $Al)_3(Al,Si)_4O_{10}(OH)_2$. This clay possesses a high cation exchange capacity (typically between 100 mmol/100 g and 150 mmol/100 g) and consequently absorbs a high amount of metal cations such as Ag^+ and Cu^{2+} and, in turn, makes very effective antibacterial metallic nanoparticles on the surface or interlamellar space of vermiculite (Drelich *et al.*, 2011). For instance, copper/vermiculite possesses high antibacterial activity against *Staphylococcus aureus*, and likely for silver/vermiculite against *Klebsiella pneumoniae* and *Pseudomonas aeruginosa* (Valášková *et al.*, 2010; Drelich *et al.*, 2011). Due to lack of information on the utilization feasibility of silver-impregnated vermiculite through scaled-up water purification system, the present study combined the antimicrobial properties of silver with high cation exchange capacity and large surface area of vermiculite (i.e., silver-impregnated vermiculite) to assess the potential antimicrobial effectiveness of the silver-impregnated vermiculite by a household water filtration system. Moreover, given that silver could moderately release from the silver-impregnated vermiculite into the water, acid-activated vermiculite was separately applied to reabsorb the released silver and enhance purification properties.

Materials and methods

Preparation and acid treatment of vermiculite

Exfoliated vermiculite (with 6-9 mm particle size and chemical composition of 37.783 wt.% SiO_2, 16.505 wt.% Al_2O_3, 15.366 wt.% Fe_2O_3, 13.151 wt.% MgO, 6.281 wt.% K_2O, 2.286 wt.% TiO_2, 1.102 wt.% Cl, 0.61 wt.% CaO, 0.077 wt.% Rb, 0.039 wt.% P_2O_5, and 6.8 wt.% the others) was purchased from Rahpouyan lidoma mineral and industrial Co., Tehran, Iran. The clay mineral was sieved to remove dust and washed several times with distilled water and dried at 80ºC for 24 h, and then dispersed into the hydrochloric acid (37% HCl, Scharlau) to leach interlayer cations and in turn to increase ion-exchange capacity. Two types of acid-treated vermiculite were prepared; two equal amounts (1100 g) of vermiculite were separately dispersed into 10 L of 1 and 2 M HCl for 6 h at room temperature. After the reaction, the acidified samples were filtered and washed several times again with distilled water to remove chlorides and

[DOR: 20.1001.1.15622916.2020.19.6.30.2]

then dried at 80ºC overnight. For simplification, hereafter the samples treated with 1 and 2 M HCl were denoted as "Verm-A" and "Verm-B", respectively.

Silver-vermiculite hybridization

To prepare the silver-impregnated vermiculite, silver nitrate ($AgNO_3$; with the purity of 99.99%) solution was applied as the precursor to load the Verm-B with silver ions. Different $AgNO_3$ solutions (0, 500, 1000, 2000 mg L^{-1}) were prepared in deionized water. The hybridization of silver with vermiculite was performed at 25ºC in dark plastic vessels through separately dispersing 270 g of Verm-B into 5 L of the $AgNO_3$ solutions for 24 h, and then the suspensions were stirred for 4 h intervals. The final hybridized Verm-B products were washed several times with deionized water to remove the loosely attached nitrate ions and dried at 80ºC. The hybridized materials and their annotations are specified in Table 1.

Table 1: Silver-impregnated vermiculites used in this study and their annotations.

Products	Description of products
Verm-B_0	Verm-B suspended only in deionized water for 24 h
Verm-B_{500}	Verm-B suspended in 500 mg L^{-1} AgNO3 solution for 24 h
Verm-B_{1000}	Verm-B suspended in 1000 mg L^{-1} AgNO3 solution for 24 h
Verm-B_{2000}	Verm-B suspended in 2000 mg L^{-1} AgNO3 solution for 24 h

Characterization of silver-impregnated vermiculite

Silver content of the hybridized materials was determined using a flame atomic absorption spectrometer (AAS) (GBC SavantAA, Australia). An amount of 1 g of the hybrid materials was thermally dissolved in Nitric acid (65% HNO_3) and the solutions were filled up into the volumetric flasks for the desired analysis. Silver standard solution for AAS was Merck (1000 mg L^{-1}, Titrisol® standard, plastic ampoule, 1.09906.0001) and the applied HNO_3 was suprapure grade Merck. Distilled water was used for all dilutions. The morphology of the hybridized products was observed with scanning electron microscopy (SEM; XL30 Philips, Netherland). SEM mapping and energy dispersive X-ray spectroscopy (EDX) analysis were also employed, respectively, to illustrate the spatial distribution of silver and to analyze the elements composition of the hybridized products.

Water filtration design

To achieve the above mentioned objectives of the experiment, four 4-stage scale-up water filtration systems were designed (Fig. 1).

[DOR: 20.1001.1.15622916.2020.19.6.30.2]

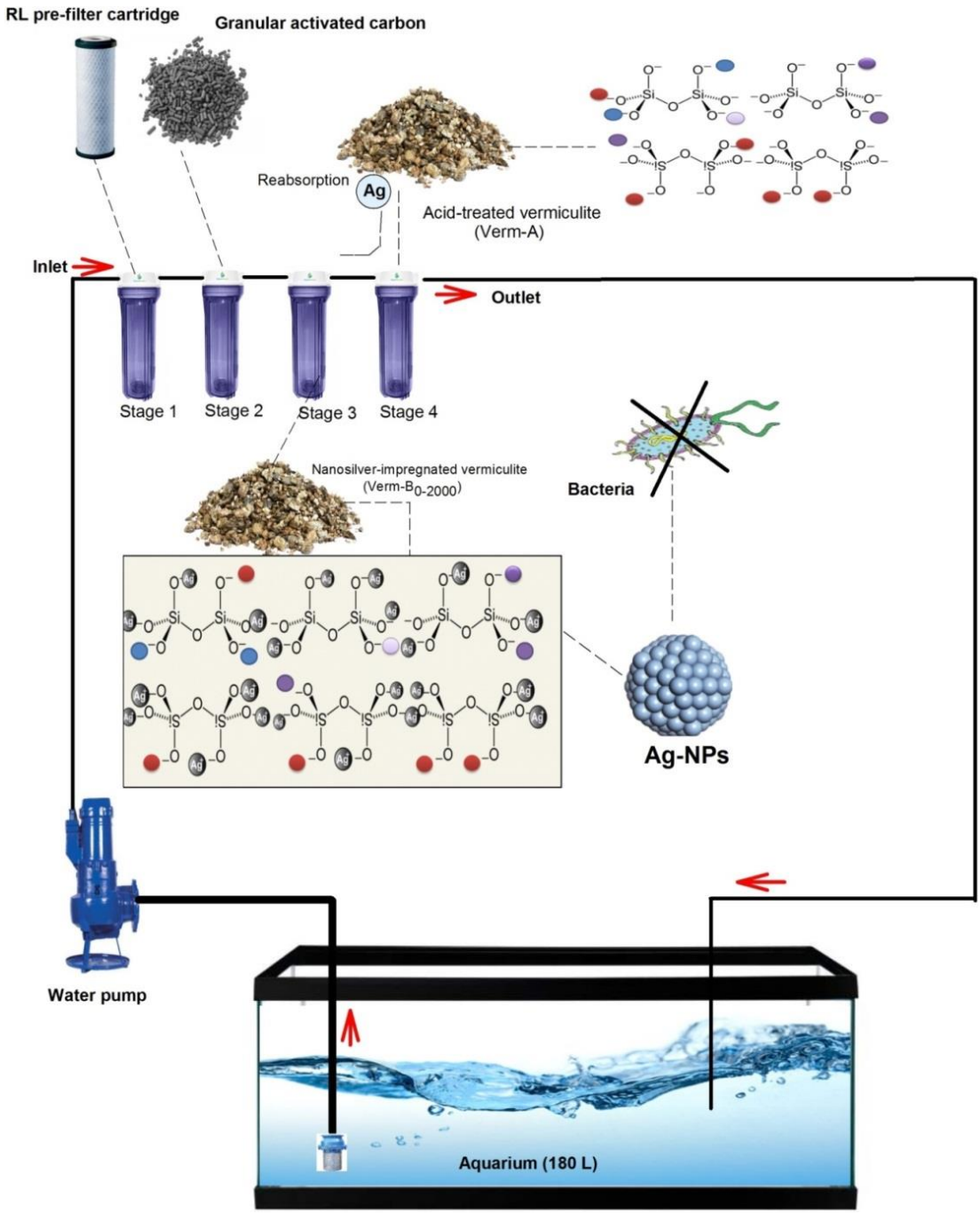

Figure 1: Schematic drawing of a four 4-stage scale-up water filtration system used to evaluate antimicrobial efficiency of the silver-impregnated vermiculites (Verm-$B_{0\text{-}2000}$) and to assess the silver removal capability of the acid-treated vermiculites (Verm-A).

For each stage, a commercial filtration cartridge was put into the water filtration housing units and filled with the desired materials as follows: stage 1, RL pre-filter cartridge to filter small particles bigger than 50 µm; stage 2, granular activated carbon (AC; 340 g) as a substrate commonly used in household filtration systems; stage 3, Verm-B (160 g) as the antimicrobial

[DOR: 20.1001.1.15622916.2020.19.6.30.2]

substrate; and stage 4, Verm-A (160 g of vermiculite only treated with 1 M HCl for reabsorbing the released Ag from stage 3). The materials used in stage 1, 2 and 4 were the same as their corresponding stage in all four filtration systems, and only the silver-impregnated vermiculites (Verm-$B_{0\text{-}2000}$) applied in stage 3 were different in terms of Ag concentration. The filtration system with Verm-B_0 was used as the control. Finally, four individual circulation systems were assembled, and each one was comprised of a water pump, a 200-liter glass aquarium (unsterilized tap water of 180 liters), and one of the designed 4-stage scale-up water filters. Outlet flow rate of ~1.7 L min^{-1} was chosen to practically assess the adherence of silver particles on the Verm-$B_{500\text{-}2000}$ surface when exposed to a higher water pressure than that of household filtration systems. To ensure water suction throughout the aquarium and avoid water lagging, the inlet collecting pipe (i.e., the pipe through which water was pumped) was set at the bottom of the aquaria. Then, the outlet water passed through stage 1, 2, 3, and 4 of the filtration system (i.e., RL pre-filter cartridge, granular activated carbon, Verm-B, and Verm-A, respectively) and finally introduced back into the aquarium. The whole designed filtration systems with Verm-B_0, Verm-B_{500}, Verm-B_{1000}, and Verm-B_{2000} were hereafter denoted as "F-B_0", "F-B_{500}", "F-B_{1000}", and "F-B_{2000}", respectively.

Antibacterial tests

To evaluate the antimicrobial effectiveness of each designed filtration system, the test was performed using bacterium *Aeromonas hydrophila* (ATCC 7965 Pasteur Institute of Iran). Bacterial suspension (10^6 CFU/mL) was inoculated into the aquaria, and then the water pumps were run continuously for 96 h. The experiment was carried out under a 12 h: 12 h light: dark cycle condition and at 24.1±1.52°C. Some physiochemical parameters of the experimental tap water were measured (Table 2).

Table 2: Some physiochemical characteristics of tap water used in the experiment.

Parameter	Concentration (mg L^{-1})
Total alkalinity	332
Total ammonium	0.13
Chloride	1.67
Sodium	14.8
$CaCO_3$	107
HCO_3	324
Total organic carbon	3.1±0.8
Dissolved oxygen	7.19 ± 0.5

Filtrates were collected at 0, 2, 14, 24, 48, 72, 96 h after inoculating the bacterium. To monitor the antibacterial effectiveness of the filtration systems, the collected samples were surface-plated onto the plate count agar (PCA). Total colony forming units (CFU) per plate were enumerated following incubation for 48 h at 36°C. The percent reduction of CFU efficiency (formula 1) and the percent of antibacterial efficiency (formula 2) were calculated on the basis of the CFU counts of bacteria in the control filtrate

[DOR: 20.1001.1.15622916.2020.19.6.30.2]

and the initial inoculated bacterial concentration, respectively (Savchenko, 2017).

(1) Efficiency (%) = (CFU in Control filtrate – CFU in silver-treated filtrate)/CFU in Control filtrate × 100

(2) Efficiency (%) = (1 - bacterial concentration in filtrate/ initial inoculated bacterial concentration) ×100

Silver detection in filtered water

To determine Ag concentration in the filtered water, triplicate samples were taken at 0, 2, 14, 24, 48, 72, 96 h during the experiment and acidified using HCl. Due to low concentration of Ag in the filtered water samples, graphite furnace (GF) analysis was carried out using the above mentioned atomic absorption spectrophotometer, coupled with a graphite tube atomizer. The above mentioned silver standard solution was used as well (see the characterization of silver-impregnated vermiculite).

Silver reabsorption

To reabsorb the released Ag from the stage 3 of all designed filtration systems (i.e., Verm-$B_{0\text{-}2000}$), Verm-A (160 g of acid activated vermiculite) was used into a cartridge in the stage 4. At the end of the experiment, the reabsorbed Ag concentrations by Verm-A were determined using the same as the procedure described for Verm-B substrates (see characterization of silver-impregnated vermiculite). Furthermore, owing to its adsorption capability for metals (Kobya *et al.*, 2005), the applied activated carbon (stage 1) was also evaluated regarding its silver content based on the same method used for Verm-A.

Results

Chemical and optical characteristics of silver-impregnated vermiculite

Silver content of the silver-hybridized Verm-B products prior to using in filtration systems is presented in Table 3. The AAS data demonstrated that the amount of silver increased following increasing $AgNO_3$ concentration, albeit in nonlinear form; the maximum silver adsorption (49.17 mg/g) was occured by Verm-B_{2000}.

Table 3: Silver content in the silver-impregnated vermiculites from a flame atomic absorption spectrometer (AAS) measurement.

Products	Ag concentration (mg/g)
Verm-B_0	0.39
Verm-B_{500}	18.75
Verm-B_{1000}	30.78
Verm-B_{2000}	49.17

SEM micrographs revealed a heterogeneous distribution of silver nanoparticles (Ag-NPs) on the surface of Verm-B_{2000} with larger Ag-NPs compared to that of Verm-B_{500} and Verm-B_{1000} (Fig. 2); the Ag-NPs average size was with the order of Verm-B_{2000} (274.808 nm)> Verm-B_{500} (194 nm)> Verm-B_{1000} (162.258 nm) (Fig. 3).

[DOR: 20.1001.1.15622916.2020.19.6.30.2]

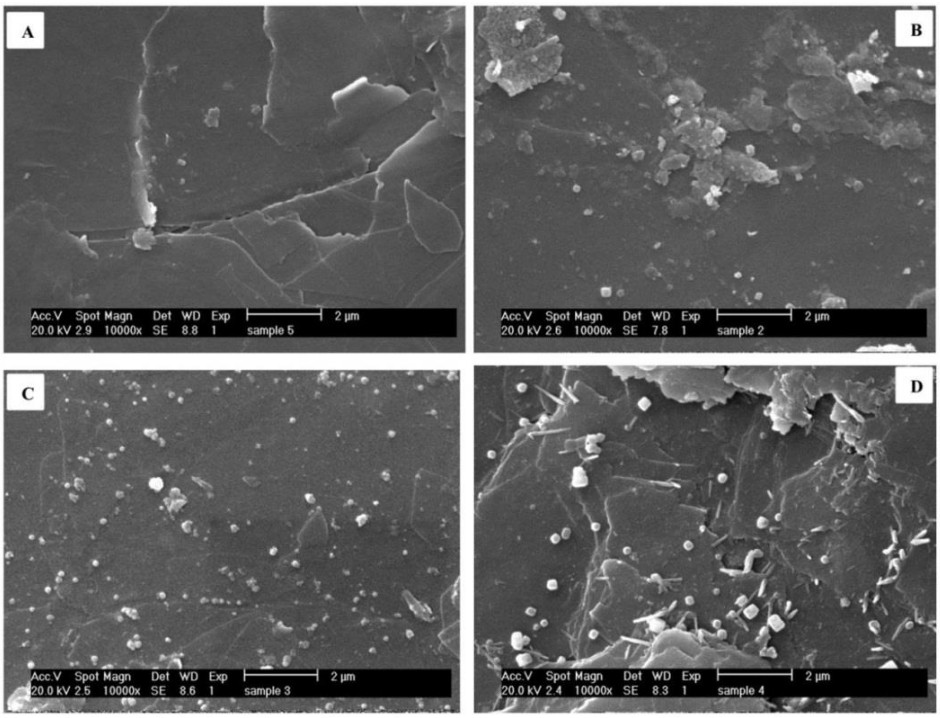

Figure 2: Scanning electron microscopy (XL30 Philips, Netherland) micrographs of Verm-B_0 (A), Verm-B_{500} (B), Verm-B_{1000} (C), and Verm-B_{2000} (D) samples decorated with silver nanoparticles.

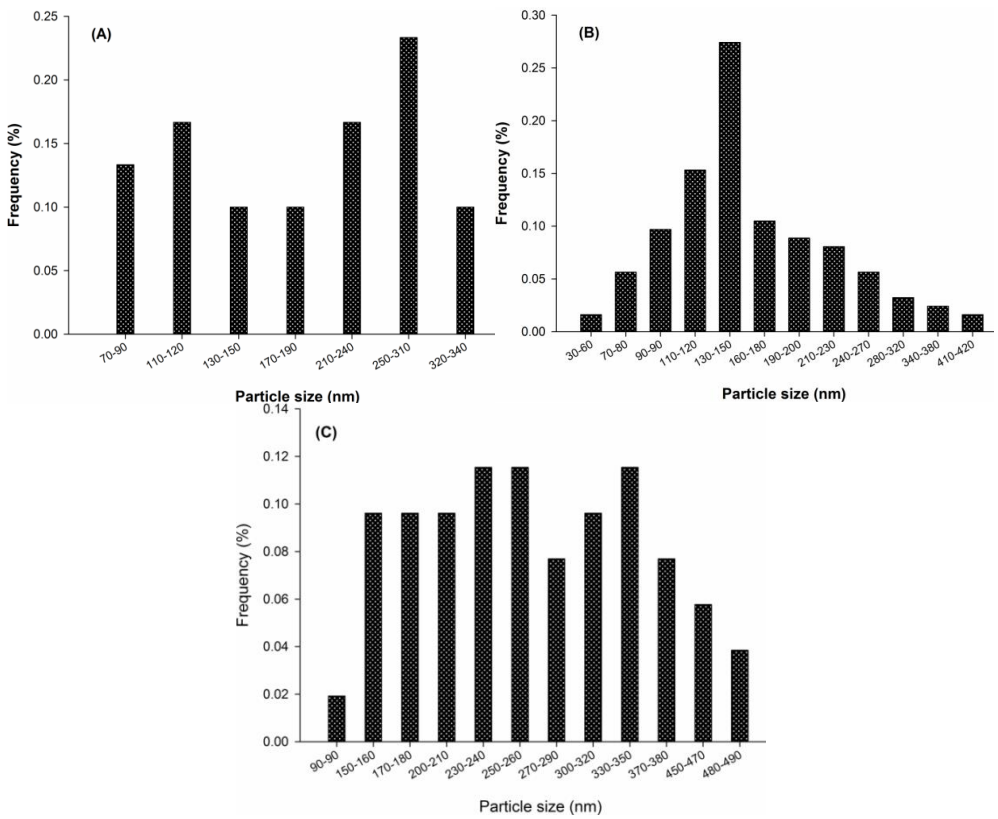

Figure 3: Size distribution of silver nanoparticles on the surface of vermiculite: Verm-B_{500} (A), Verm-B_{1000} (B), and Verm-B_{2000} (C) prepared using 500, 1000, and 2000 mg L^{-1} of silver nitrate solutions, respectively.

[DOR: 20.1001.1.15622916.2020.19.6.30.2]

SEM mapping demonstrated uniformly distribution of silver on the layers of the vermiculites hybridized in 500 and 1000 mg L^{-1} $AgNO_3$ solutions, but heterogeneously that of in 2000 mg L^{-1} (Fig.4). Furthermore, the qualitative elemental composition of the Verm-B products and the as-received exfoliated vermiculite (raw Verm) was determined by SEM–EDX mapping (Table 4). The elemental analysis revealed the highest amount of Ag (4.21 wt%) in Verm-B_{2000} and the lowest in Verm-B_0 (not detected), which are in line with the results of AAS analysis (see Table 3). In terms of weight-percent (wt%), acid treatment of the raw Verm with 2M HCl caused partial alterations in its elements composition; the content of Si and Ca decreased, whereas the other components increased. However, the vermiculites treated with 2M HCl into $AgNO_3$ solutions gave rise to a dose-dependent decrease in the weight percent of Mg, Al, Si, K, and Cl but a dose-dependent increase of Ca, Fe, and Na. The data also revealed that the content of Ti and Cl disappeared completely after 24 h dispersing into the applied $AgNO_3$ solutions.

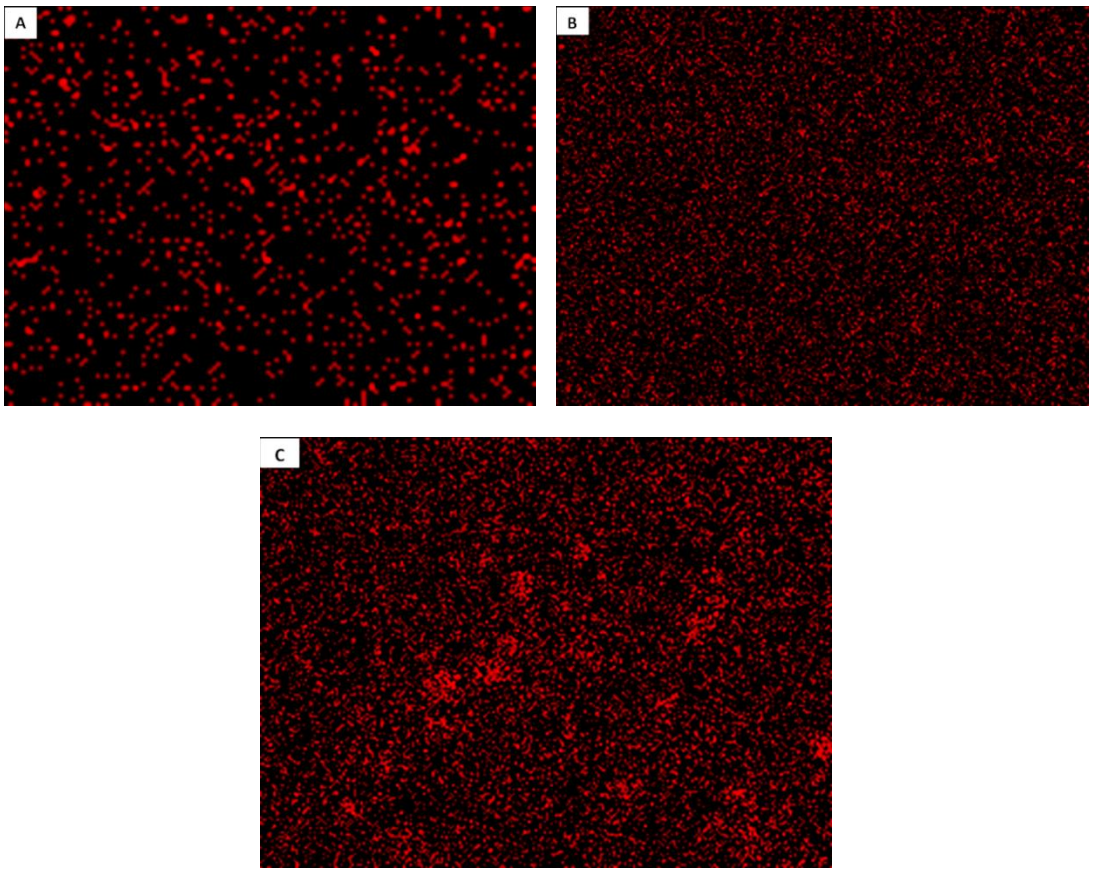

Figure 4: SEM mapping images of vermiculites decorated with different concentrations of silver; Verm-B_{500} (A), Verm-B_{1000} (B), and Verm-B_{2000} (C) prepared using 500, 1000, and 2000 mg L^{-1} of silver nitrate solutions, respectively. Red color is corresponding elemental mapping for silver or silver nanoparticles (Ag-NPs).

[DOR: 20.1001.1.15622916.2020.19.6.30.2]

Table 4: The main elemental composition of the silver-impregnated Verm-B products from EDX measurement.

Sample	Main elemental composition (wt%)									
	Ag	Mg	Al	Si	K	Ca	Ti	Fe	Na	Cl
Raw Verm**	n.d*	7.20	11.80	38.97	9.68	0.93	1.36	28.60	0.33	1.13
Verm-B_0	n.d*	8.44	12.15	30.64	9.90	0.81	2.91	28.74	2.22	4.19
Verm-B_{500}	1.28	8.14	13.64	35.05	12.18	0.22	n.d*	28.96	0.53	n.d*
Verm-B_{1000}	3.53	7.53	13.10	32.62	13.33	0.42	n.d*	28.72	0.75	n.d*
Verm-B_{2000}	4.21	7.07	12.02	30.22	10.89	1.16	n.d*	32.96	1.47	n.d*

* n.d. is the abbreviation of "not detected".
** "Raw Verm" is the as-received exfoliated vermiculite without acid treatment.

Antibacterial efficiency

Figure 5 demonstrates the total bacterial count after inoculating of 10^6 CFU mL^{-1} *A. hydrophila* into the water filtration systems. The bacterial population was significantly decreased in the first two hours of the experiment, even in the control system in which bacteria were also reduced by more than 59.82% in the beginning but the efficiency rapidly dropped. Following 96 h dynamic flow, the time-kill test showed the high capability of the silver-impregnated vermiculite for killing total bacteria or inhibiting the bacterial growth, with reducing the bacterial growth over 95% in all of the filtration systems containing Verm-$B_{500\text{-}2000}$. F-B_{1000} showed the highest log reduction value of 3.47 CFU mL^{-1} at 96 h when compared to F-B_0 at the time-matched point. The antibacterial efficiency dropped as F-B_0 (518.32%)> B_{500} (22.6%)> F-B_{2000} (9.18%)> F-B_{1000} (0.77%) (Fig. 6).

Silver release and silver reabsorption efficiency

The amount of silver in the filtrated water demonstrated different levels during a 96 h dynamic-flow test (Fig. 7). At the first two hours of the experiment, the concentration of silver in filtrated water in F-B_{2000} (0.801 ug/L) and F-B_{500} (0.678 ug/L) showed significantly higher amounts than that of in F-B_{1000} (0.392 ug/L), but over time decreased close to F-B_0 (control treatment). However, filtrated water in F-B_{1000} displayed almost a constant concentration of silver over the experiment.

The amount of silver reabsorbed by Verm-A in the stage 4 and activated carbon in the stage 1 is shown in Table 5. Verm-A revealed high capability to reabsorb the released silver from stage 3; the amount of absorbed silver by Verb-A was about 3-10 times more than that of the applied activated carbon. The percentage of silver released from the total Ag in Verm-B_{500} was 32.36%, Verm-B_{1000} 27.87%, and Verm-B_{2000} 17.24%; of these amounts, respectively, 90.9%, 81.8%, and 75.7% were reabsorbed by Verm-A.

[DOR: 20.1001.1.15622916.2020.19.6.30.2]

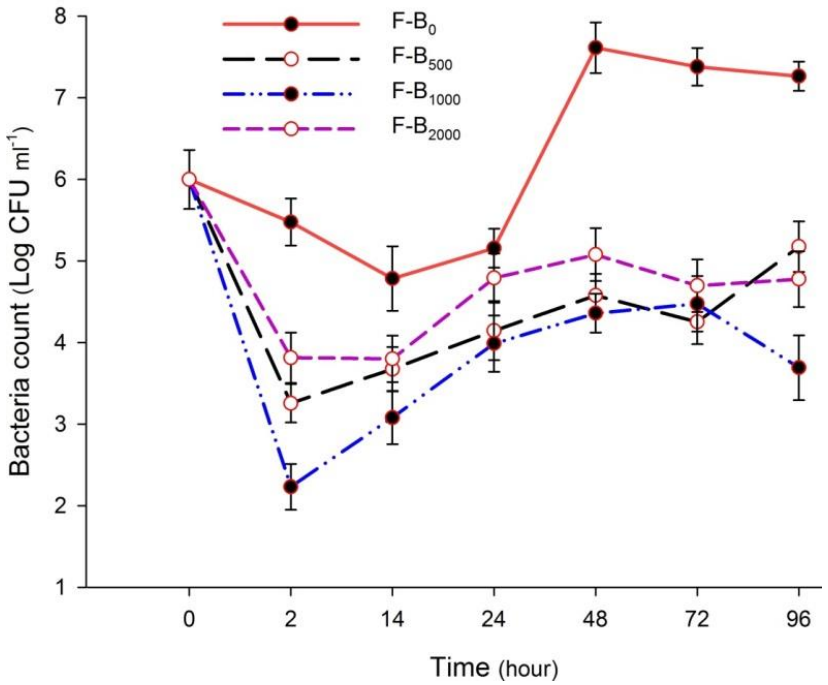

Figure 5: Total bacterial growth after inoculation of 10^6 CFU mL^{-1} *A. hydrophila* into the water filtration systems (F-B_0, F-B_{500}, F-B_{1000}, and F-B_{2000}) containing vermiculites impregnated with different silver contents. Water filtrated samples were collected during 96 h from dynamic flow systems.

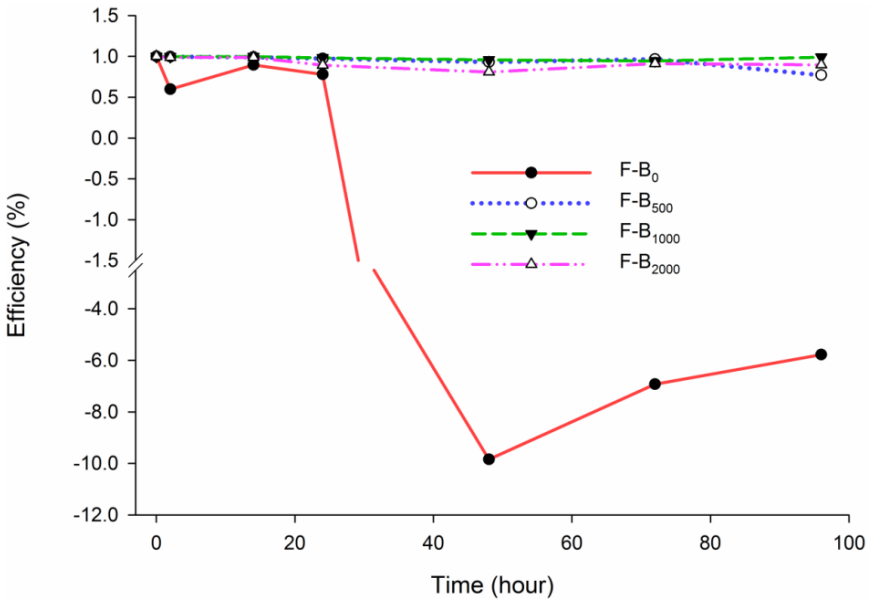

Figure 6: Anti-bacterial efficiency (%) of water filtration systems (F-B_0, F-B_{500}, F-B_{1000}, and F-B_{2000}) containing vermiculites impregnated with different silver contents. Water filtrated samples were collected during 96 h from dynamic flow systems.

[DOR: 20.1001.1.15622916.2020.19.6.30.2]

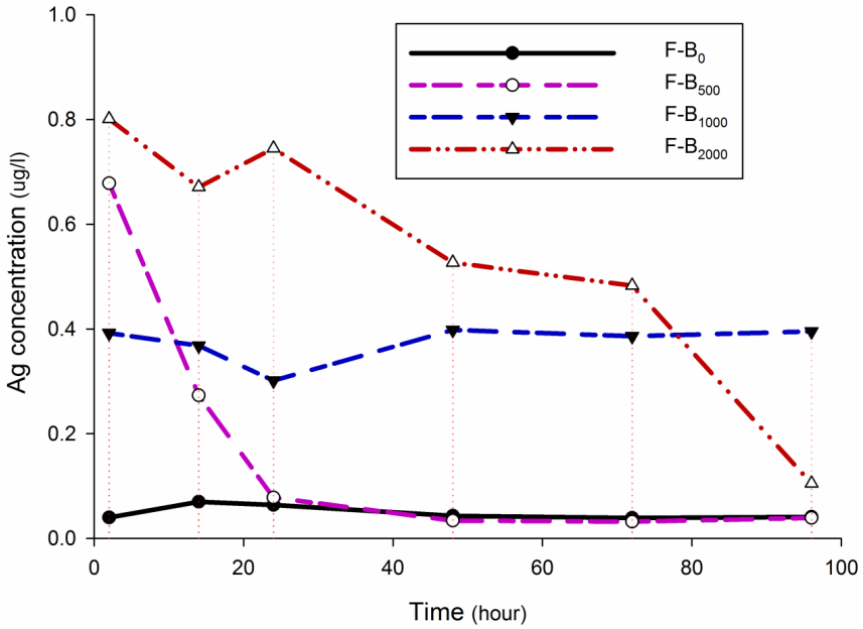

Figure 7: Silver released into water filtration systems (F-B_0, F-B_{500}, F-B_{1000}, and F-B_{2000}) containing vermiculites impregnated with different silver contents. Water filtrated samples were collected during 96 h from dynamic flow tests.

Table 5: Silver concentrations reabsorbed by acid activated vermiculite (Verm-A) and activated carbon (AC) following incorporation in water filtration systems (F-B_0, F-B_{500}, F-B_{1000}, and F-B_{2000}) containing vermiculites impregnated with different silver contents.

Water filtration systems	Silver concentration (mg/g)	
	Verm-A	AC
F-B_0	0.378 ±0.0031	0.097±0.006
F-B_{500}	5.52± 0.46	0.26±0.023
F-B_{1000}	7.025±0.133	0.732±0.0321
F-B_{2000}	6.42±0.17	0.969±0.0137

Discussion

The incorporation of Ag^+ or Ag-NPs into the low-cost materials has strengths (cost effectiveness, easy availability and consumption of minimal electricity) and weaknesses (necessity of surface-coating techniques and depletion of silver from the surface). Such restrictions indicate that low-cost, easily scalable, aqueous compatible and potentially environmental friendly methods could provide nanoparticles suitable for water technology (Chan *et al.*, 2009; Praveena and Aris, 2015; Simeonidis *et al.*, 2016). Traditionally, acid activation of clay materials is a chemical treatment to obtain materials with enhanced surface properties suitable for new applications or display an interesting new behaviour. Acid activation lixiviates cations from clay minerals and in turn enhances their overall negative charge (Komadel, 2016; Wang *et al.*, 2016; Valášková *et al.*, 2018). The quantitative and qualitative analysis by AAS, SEM and

[DOR: 20.1001.1.15622916.2020.19.6.30.2]

SEM–EDX mapping confirmed that the acid activated vermiculites (i.e., Verm-B) have a potential capability to be impregnated with silver. However, there is an optimal ration of Ag-NPs that can be decorated on a given amount of Verm-B. The results are supported by previous study which applied 0.01 mol L^1 $AgNO_3$ aqueous solution to prepare silver/vermiculites and silver/montmorillonites through only cation exchange process (Valášková *et al.*, 2010), although the present study used acid activated vermiculite to be impregnated with silver. In addition, SEM images revealed silver with nano dimension crystallites on the surface of Verm-B products which had been exposed to the $AgNO_3$ solutions. The silver crystallization could be strengthened by studies of the other researchers who applied negative zeta potential of vermiculite to precipitate metal ions such as silver and copper into the nano scales (Magana *et al.*, 2008; Drelich *et al.*, 2011; Hundáková *et al.*, 2014, Valášková *et al.*, 2018).

EDX mapping of the silver-impregnated vermiculites (Verm-$B_{500-2000}$) exhibited a dose-dependent decrease in the weight percent of Mg^{2+}, Al^{+3}, Si^{+2},K^+, and Cl^- after dispersion into the $AgNO_3$ solutions. This change in chemical composition could be ascribed to the silver cation exchange and reduced metallic silver in octahedral and tetrahedral sheets of the Verm-B products. These data conforms to the study reported by Valášková (2010) who demonstrated Na^+, K^+, Ca^{2+}, and Mg^{2+} releasing from vermiculite and montmorillonite after ion exchange with $AgNO_3$ solution.

The present study showed strong antibacterial efficiency (over 95%) of the designed filtration systems with silver-impregnated Verm-B products, with the highest log reduction value of 3.47 CFU mL^{-1} for F-B_{1000}. High bactericidal activity of the developed vermiculite suggested that it might be a good candidate for broad applications, especially purify water contaminated with bacteria. In addition, the slight observed reduction in the antibacterial efficiency after 96 h filtration suggested a long life span for the filtration systems.

Many studies demonstrated that the bactericidal activity of Ag-NPs is a size-dependent interaction with bacteria (Pal *et al.*, 2007; Usha *et al.*, 2018). Hence, the observed higher antibacterial effectiveness of F-B_{1000} could be ascribed to the smaller size and larger surface area of Ag-NPs and their homogeneous distribution on Verm-B_{1000} compared to Verm-B_{500} and Verm-B_{2000}. Similar result has been reported by Benhacine (2016) who showed that uncontrolled size and heterogeneity of Ag-NPs in polymer composites reduce the point-of-time biocidal performance of the materials. Other researchers have also reported similar strong antibacterial activity for vermiculite and montmorillonite which were decorated with copper and silver (Magana *et al.*, 2008; Drelich *et al.*, 2011; Xu *et al.*, 2011).

[DOR: 20.1001.1.15622916.2020.19.6.30.2]

In comparison with F-B_{500} and F-B_{2000}, the rate of silver released into the filtrated water in F-B_{1000} demonstrated a constant concentration, suggesting that the smaller size of Ag-NPs in Verm-B_{1000} led to a moderate migration of silver into the water. That is, the observed differences in size distribution of Ag-NPs could be an explanatory reason over insufficient adherence of Ag-NPs at the Verm-B surface, which is confirmed by Valášková (2010). In addition, there is an optimal ration of silver that can be coated on a given amount of acid-activated vermiculite due to constraints on the limited negative charges of the activated vermiculites that silver can be deposited on. Thus, the additional Ag^{+} or larger Ag-NPs on the surface of the vermiculite layers could be removed by water flow in the filtration systems.

Due to having unique physicochemical properties such as high cation exchange capacity and high specific surface area, clay minerals especially vermiculite or montmorillonite are affordable adsorbents for the removal of metal ions to prevent contamination of aquatic and soil systems by leachates or industrial wastewaters (Stylianou *et al.*, 2007; Abollino *et al.*, 2008: Malamis and Katsou, 2013; Cantuaria *et al.*, 2016; do Nascimento *et al.*, 2016). Acid-activated clays possess high overall negative zeta potential (i.e., net negative charges) which facilitates ion exchange and increases their capacity to absorb cations, such as metal ions. The acid-leached cations, such as Mg^{2+}, Al^{+3}, Si^{+2}, and K^{+}, are easily replaced by those with close atomic radii and equivalent charge in the interlayer regions of vermiculite (Drelich *et al.*, 2011; Hashem *et al.*, 2015; Komadel, 2016; do Nascimento *et al.*, 2016; Klika *et al.*, 2017). In the present study, the acid activated vermiculite (i.e., Verm-A) displayed a critical function to reabsorb high levels (75%-90%) of the released silver from the silver-impregnated vermiculites (Verm-B_{500}, Verm-B_{1000}, and Verm-B_{2000}). Similar results have been reported by Stylianou (2007) and Cantuaria (2016) who verified high capacities of bentonite and exfoliated vermiculite as adsorbents for silver and copper from aqueous solutions, respectively.. In addition, the removal rate of metal ions by clay minerals is quite rapid and maximum adsorption occurs within the first hours of contact (Kocaoba *et al.*, 2007). For this reason, the observed rapid reduction of silver concentration in filtrated water, especially in F-B_{500} and F-B_{2000}, could be attributed to the high potential capability of Verm-A for reabsorbing the escaped silver.

Overall, this study is a proof-of-concept example of water purification system using vermiculite embedded with Ag-NPs and acid-activated vermiculite. The data demonstrated that these nanoscale particles can be prepared cost-effectively with respect to the increase in supplied water price for consumers. The Ag-NPs loaded vermiculites showed interesting

[DOR: 20.1001.1.15622916.2020.19.6.30.2]

antibacterial activity. The antibacterial activity besides high reabsorption capability of acid-activated vermiculite (Verm-A) to released silver is a promising feature for water disinfection and purification. Hence, the observed bactericidal efficiency in the filtration systems and the amounts of silver released into the filtrated water could open an opportunity to use silver-impregnated Verm-B in water treatment field, especially for the outdoors circumstances. Moreover, the Verm-A could be introduced as an affordable absorbent for silver removal from industrial wastewaters and reduce environmental contamination. However, making an electrostatic attraction between Ag-NPs and Verm-B using binding agents could be an effective treatment to reduce the amount of released silver.

Acknowledgment

The authors gratefully acknowledge the support of the Tarbiat Modares University which funded this research.

References

Abebe, L.S., Chen, X. and Sobsey, M.D., 2016. Chitosan coagulation to improve microbial and turbidity removal by ceramic water filtration for household drinking water treatment. *International Journal of Environmental Research and Public Health,* 13**,** 269. DOI: 10.3390/ijerph13030269.

Abollino, O., Giacomino, A., Malandrino, M. and Mentasti, E., 2008. Interaction of metal ions with montmorillonite and vermiculite. *Applied Clay Science,* 38**,** 227-236. DOI: 10.1016/j.clay.2007.04.002.

Benhacine, F., Siham Hadj-Hamou, A. and Habi, A., 2016. Development of long-term antimicrobial poly (ε-caprolactone)/silver exchanged montmorillonite nanocomposite films with silver ion release property for active packaging use. *Polymer Bulletin,* 73**,** 1207-1227. DOI: 10.1007/s00289-015-1543-9.

Cantuaria, M.L., De Almeida Neto, A.F., Nascimento, E.S. and Vieira, M.G., 2016. Adsorption of silver from aqueous solution onto pre-treated bentonite clay: complete batch system evaluation. *Journal of Cleaner Production,* 112**,** 1112-1121. DOI: 10.1016/j.jclepro.2015.07.021.

Chan, L., Chan, M. and Wang, J., 2009. Design of water filter for third world countries. *Department of Mechanical and Industrial Engineering*.

Do Nascimento, F.H., De Souza Costa, D.M. and Masini, J.C., 2016. Evaluation of thiol-modified vermiculite for removal of Hg (II) from aqueous solutions. *Applied Clay Science,* 124**,** 227-235. DOI: 10.1016/j.clay.2016.02.017.

Drelich, J., Li, B., Bowen, P., Hwang, J.Y., Mills, O. and Hoffman, D., 2011. Vermiculite decorated with copper nanoparticles: Novel antibacterial hybrid material. *Applied*

[DOR: 20.1001.1.15622916.2020.19.6.30.2]

Surface Science, 257**,** 9435-9443. DOI: 10.1016/j.apsusc.2011.06.027.

Fewtrell, L., Majuru, B. and Hunter, P.R., 2017. A re-assessment of the safety of silver in household water treatment: rapid systematic review of mammalian in vivo genotoxicity studies. *Environmental Health,* 16**,** 66. DOI:10.1186/s12940-017-0279-4.

Hashem, F., Amin, M. and El-Gamal, S., 2015. Chemical activation of vermiculite to produce highly efficient material for Pb2+ and Cd2+ removal. *Applied Clay Science,* 115**,** 189-200. DOI: 10.1016/j.clay.2015.07.042.

Hundáková, M., Valášková, M., Samlíková, M. and Pazdziora, E., 2014. Vermiculite with ag and cu used as an antibacterial nanofiller in polyethylene. *GeoScience Engineering,* 60**,** 28-36. p. 28-36, ISSN 1802-5420.

Khan, M.A. and Ahmad, A.M.A., 2016. Assessment of household water tanks microbial quality in Dubai, United Arab Emirates. DOI: 10.4491/eer.2016.051.

Kirby, M.A., Nagel, C.L., Rosa, G., Umupfasoni, M.M., Iyakaremye, L., Thomas, E.A. and Clasen, T.F., 2017. Use, microbiological effectiveness and health impact of a household water filter intervention in rural Rwanda—A matched cohort study. *International Journal of Hygiene and Environmental Health.* 220(**6**), 1020-1029. DOI: 10.1016/j.ijheh.2017.05.013.

Klika, Z., Seidlerová, J., Kolomazník, I. and Hundáková, M., 2017. Vermiculite as efficient sorbent of CeIII and CeIV. *Environmental Chemistry,* 14**,** 39-47. DOI: 10.1071/EN16112.

Kobya, M., Demirbas, E., Senturk, E. and Ince, M., 2005. Adsorption of heavy metal ions from aqueous solutions by activated carbon prepared from apricot stone. *Bioresource Technology,* 96**,** 1518-1521. DOI: 10.1016/j.biortech.2004.12.005.

Kocaoba, S., Orhan, Y. and Akyüz, T., 2007. Kinetics and equilibrium studies of heavy metal ions removalby use of natural zeolite. *Desalination,* 214**,** 1-10. DOI: 10.1016/j.desal.2006.09.023.

Komadel, P., 2016. Acid activated clays: Materials in continuous demand. *Applied Clay Science,* 131**,** 84-99. DOI: 10.1016/j.clay.2016.05.001.

Lantagne, D., Klarman, M., Mayer, A., Preston, K., Napotnik, J. and Jellison, K., 2010. Effect of production variables on microbiological removal in locally-produced ceramic filters for household water treatment. *International Journal of Environmental Health Research,* 20**,** 171-187. DOI: 10.1080/09603120903440665.

Magana, S., Quintana, P., Aguilar, D., Toledo, J., Angeles-Chavez, C., Cortes, M., Leon, L., Freile-Pelegrín, Y., Lopez, T. and

[DOR: 20.1001.1.15622916.2020.19.6.30.2]

Sánchez, R.T., 2008. Antibacterial activity of montmorillonites modified with silver. *Journal of Molecular Catalysis A: Chemical,* 281**,** 192-199. DOI: 10.1016/j.molcata.2007.10.024.

Malamis, S. and Katsou, E., 2013. A review on zinc and nickel adsorption on natural and modified zeolite, bentonite and vermiculite: Examination of process parameters, kinetics and isotherms. *Journal of Hazardous Materials,* 252**,** 428-461. DOI: 10.1016/j.jhazmat.2013.03.024.

Noubactep, C., Caré, S., Togue-Kamga, F., Schöner, A. and Woafo, P., 2010. Extending service life of household water filters by mixing metallic iron with sand. *Clean–Soil, Air, Water,* 38**,** 951-959. DOI: 10.1002/clen.201000177.

Pal, S., Tak, Y.K. and Song, J.M., 2007. Does the antibacterial activity of silver nanoparticles depend on the shape of the nanoparticle? A study of the gram-negative bacterium Escherichia coli. *Applied and Environmental Microbiology,* 73**,** 1712-1720. DOI: 10.1128/AEM.02218-06.

Pompei, C.M., Ciric, L., Canales, M., Karu, K., Vieira, E.M. and Campos, L.C., 2017. Influence of PPCPs on the performance of intermittently operated slow sand filters for household water purification. *Science of The Total Environment,* 581**,** 174-185. DOI: 10.1016/j.scitotenv.2016.12.091.

Praveena, S.M. and Aris, A.Z., 2015. Application of low-cost materials coated with silver nanoparticle as water filter in Escherichia coli removal. *Water Quality, Exposure and Health,* 7**,** 617-625. DOI: 10.1007/s12403-015-0167-5.

Qu, X., Alvarez, P.J. and Li, Q., 2013. Applications of nanotechnology in water and wastewater treatment. *Water research,* 47**,** 3931-3946. DOI: 10.1016/j.watres.2012.09.058.

Savchenko, O., 2017. Application of low intensity pulsed ultrasound for microbial cell stimulation in bioprocesses and development of carbon-based silver covered filters for microbial cells removal in water systems. University of Alberta. DOI: 10.7939/R3VM4387J.

Simeonidis, K., Mourdikoudis, S., Kaprara, E., Mitrakas, M. and Polavarapu, L., 2016. Inorganic engineered nanoparticles in drinking water treatment: a critical review. *Environmental Science: Water Research and Technology,* 2**,** 43-70. DOI: 10.1039/C5EW00152H.

Singer, S., Skinner, B. and Cantwell, R.E., 2017. Impact of surface maintenance on BioSand filter performance and flow. *Journal of Water and Health,* 15**,** 262-272. DOI: 10.2166/wh.2017.129.

Stylianou, M.A., Inglezakis, V.J., Moustakas, K.G., Malamis, S.P. and Loizidou, M.D., 2007. Removal of Cu (II) in fixed bed and batch reactors using natural zeolite and exfoliated vermiculite as adsorbents.

[DOR: 20.1001.1.15622916.2020.19.6.30.2]

Desalination, 215**,** 133-142. DOI: 10.1016/j.desal.2006.10.031.

Usha, M., Thirumagal, J. and Mahegeswari, R., 2018. A Study on Silver Nano-Particle Production from Aristolochia Bracteata and Its Antimicrobial Activity.

Valášková, M., Hundáková, M., Kutláková, K.M., Seidlerová, J., Čapková, P., Pazdziora, E., Matějová, K., Heřmánek, M., Klemm, V. and Rafaja, D., 2010. Preparation and characterization of antibacterial silver/vermiculites and silver/montmorillonites. *Geochimica et Cosmochimica Acta,* 74**,** 6287-6300. DOI: 10.1016/j.gca.2010.08.025.

Valášková, M., Kupková, J., Martynková, G.S., Seidlerová, J., Tomášek, V., Ritz, M., Kočí, K., Klemm, V. and Rafaja, D., 2018. Comparable study of vermiculites from four commercial deposits prepared with fixed ceria nanoparticles. *Applied Clay Science,* 151**,** 164-174. DOI: 10.1016/j.clay.2017.10.006.

Wang, L., Wang, X., Yin, J. and Wang, C., 2016. Insights into the physicochemical characteristics from vermiculite to silica nanosheets. *Applied Clay Science,* 132**,** 17-23. DOI: 10.1016/j.clay.2016.05.006.

Xu, G., Qiao, X., Qiu, X. and Chen, J., 2011. Preparation and characterization of nano-silver loaded montmorillonite with strong antibacterial activity and slow release property. *Journal of Materials Science and Technology,* 27**,** 685-690. DOI: 10.1016/S1005-0302(11)60126-6.